

# Review of “Comparison of two automated aerosol typing methods and their application on an EARLINET station” by K. A. Voudouri, N. Siomos, K. Michailidis, N. Papagiannopoulos, L. Mona, C. Cornacchia, D. Nicolae, and D. Balis

As indicated by the title, this paper uses EARLINET  $3\alpha + 2\beta$  lidar measurements to compare the performance of two different aerosol typing algorithms: the Papagiannopoulos (AKA Mahalanobis distance) algorithm and the NATALI algorithm from Nicolae et al.

For the Papagiannopoulos algorithm, aerosol classes are defined using an ensemble of high quality EARLINET measurements that has been manually partitioned by subject matter experts to ensure uniformity of the optical characteristics of all observations within each class. For the Nicolae/NATALI algorithm, aerosol classes are defined using “values obtained from a specially designed aerosol model with simulations from over 50,000 synthetic cases of [*different types of*] aerosols”. Both classification schemes are trained using supervised learning techniques (although this point is not mentioned in the manuscript).

The lidar measurements used as algorithm inputs for the Papagiannopoulos algorithm are

- a) backscatter-related Ångström Exponent at 355nm and 1064nm ( $AE_{355/1064}$ ),
- b) the lidar ratio at 532 nm ( $LR_{532}$ ), and
- c) the ratio of the lidar ratios ( $LR_{532}/LR_{355}$ )

The lidar measurements used as algorithm inputs by the Nicolae/NATALI algorithm are not specified in this manuscript.

The high resolution variant of NATALI identifies 14 distinct aerosol types. The “low resolution without depolarization” variant used in this study recognizes five aerosol types: dust, smoke, continental polluted, continental, and maritime (page 6, line 15–16). For this study, the smoke and continental polluted types were combined into a single ‘polluted smoke’ type, so that only four types are recognized: dust, polluted smoke, continental, and maritime.

The standard Papagiannopoulos algorithm identifies 8 aerosol types: clean continental, polluted continental, pure dust, mixed dust (dust + maritime), polluted dust (dust + smoke and/or pollution), mixed maritime, smoke, and volcanic. For this study, these 8 types are combined to yield the same four types (page 7, line 1–2) that are recognized by the modified NATALI algorithm: dust (dust + volcanic + mixed dust + polluted dust), polluted smoke (smoke + polluted continental), clean continental, and maritime (mixed maritime).

Both algorithms were applied to the identical set of lidar measurements of 116 different aerosol layers. The NATALI algorithm successfully classified 80 of the 116 layers (~69%). The Papagiannopoulos algorithm successfully classified 114 of the 116 layers (~98%). The subsequent analyses are largely devoted to comparing classification results for the 80 cases in which both algorithms were successful.

The poor performance of the NATALI algorithm when applied to real-world lidar measurements suggests a disparity between the NATALI aerosol models and the EARLINET measurements. Similar poor performance (39% failure rate) was found in a simulation study in which the authors

used the NATALI aerosol model to generate inputs for the Papagiannopoulos algorithm. Unfortunately, the authors do not investigate the possible causes or sources of these disparities.

In its present form, I cannot recommend this manuscript for publication. Most importantly, this study does not appear to address any specific science questions. Instead, it offers a one-sided comparison between two retrieval techniques. I say one-sided because the authors' analyses are so heavily focused on those cases where both algorithms are successful. However, they have clearly demonstrated that, for given sets of inputs, both algorithms are subject to large failure rates. The underlying causes of these failures are tantalizingly interesting and, I suspect, likely to be highly informative in developing the next iteration of automated aerosol typing algorithms.

This version of the manuscript also contains a number of flaws that make it difficult to understand. For example,

- a) important terms are never defined (e.g., color ratio);
- b) terms that are defined are used inconsistently (e.g., 'Ångström exponent', which is initially defined in terms of backscatter coefficients, is used interchangeably to describe backscatter-related Ångström exponents and extinction-related Ångström exponents);
- c) the descriptions of the classification algorithms are far too brief (e.g., the description of the NATALI algorithm does not provide the level of detail required to evaluate the sensitivity study that the authors perform); and
- d) the derivation of key results is not well-explained (e.g., the calculation required to produce the numbers reported in figures 4 and 5 are not described).

Below please find an annotated version of the manuscript the contains several more detailed comments and questions.



# Comparison of two automated aerosol typing methods and their application on an EARLINET station.

Kalliopi Artemis Voudouri<sup>1</sup>, Nikolaos Siomos<sup>1</sup>, Konstantinos Michailidis<sup>1</sup>,  
Nikolaos Papagiannopoulos<sup>2,3</sup>, Lucia Mona<sup>2</sup>, Carmela Cornacchia<sup>2</sup>, Doina Nicolae<sup>4</sup>, and Dimitris Balis<sup>1</sup>

<sup>1</sup>Laboratory of atmospheric physics, Physics Department, Aristotle University of Thessaloniki, Greece

<sup>2</sup>Consiglio Nazionale delle Ricerche, Istituto di Metodologie per l'Analisi Ambientale (CNR-IMAA), Tito Scalo (PZ), Italy

<sup>3</sup>CommSensLab, Dept. of Signal Theory and Communications, Universitat Politècnica de Catalunya, Barcelona, Spain

<sup>4</sup>National Institute of R&D for Optoelectronics (INOE2000), Magurele, Romania

**Correspondence:** Kalliopi Artemis Voudouri (kavoudou@auth.gr)

**Abstract.** In this study we compare two automatic algorithms for the characterization of the aerosol layers derived from a Raman lidar and we test their application over a specific environment in continental Thessaloniki. Both automated aerosol typing methods base their typing on aerosol intensive properties. The methodologies are briefly described and the application on two case studies is presented. The results are checked for their consistency with satellite products and model simulations.

5 Further application of the two classification tools was conducted. The evaluated dataset corresponds to ACTRIS/EARLINET (European Aerosol Research Lidar NETwork) Thessaloniki data acquired during the period 2012-2015. 80 layers out of 116 (percentage of 69%) were successfully typed by both algorithms and assigned to four major types of aerosols: Dust, Maritime, PollutedSmoke and Clean Continental. The analysis showed that the two algorithms are in a very good agreement, when applied to real atmospheric conditions, with an agreement percentage of 88.8% for Dust, 93.7% for PollutedSmoke and 70%  
10 for CleanContinental. The Maritime category was the one with the largest spread. These differences are attributed to differences in defining the aerosol types for the two methods. The overall consistency of the aerosol typing between the two automatic procedures despite the different aerosol type definition, allows their applicability to lidar data for characterization purposes. The joint characterization shows the highest degree of confidence in identifying Dust and PollutedSmoke, and emphasizes the need of further investigation for Maritime and Clean Continental type.

## 15 1 Introduction

The aerosol classification is a critical topic in understanding the impact of different aerosol sources on climate, weather systems, and air quality. Thus, a number of typing schemes have been applied to classify aerosols, based on the synergistic information of the scattering mechanisms and the polarization state of the received light of different wavelengths (e.g., Ansmann and Müller, 2005). For example, Hamill et al. (2016), developed an aerosol classification scheme using the optical properties  
20 derived from the AERONET (Aerosol Robotic Network) ground-based network of sun photometers. Five types of aerosols were defined based on reference clusters, characteristic of a particular type of aerosol (i.e., Maritime, Urban Industrial, Dust, Mixed and Biomass Burning). Schmeisser et al. (2017) also, used aerosol optical properties (i.e., scattering Ångström exponent,



absorption Ångström exponent and single scattering albedo) derived from in situ measurements in order to classify aerosols. Their typing scheme was based on three different aerosol classification methods.

Active remote sensing instruments such as ground or space-based lidars, are a key technique for characterizing aerosols as they provide vertically-resolved information of extensive (e.g., aerosol backscatter coefficient, aerosol extinction coefficient and volume depolarization ratio) and intensive properties (e.g., Ångström exponent, lidar ratio and particle depolarization ratio) of different aerosol types. The intensive properties are type sensitive and provide separate classification for each detected layer (e.g., Müller et al., 2007; Ansmann et al., 2011; Tesche et al., 2011; Burton et al., 2012; Pappalardo et al., 2013; Groß et al., 2013; Amiridis et al., 2015; Giannakaki et al., 2015; and Baars et al., 2016).

Aerosol typing schemes have been developed for high-resolution lidar measurements of space-borne lidars (e.g., CALIPSO, Cloud-Aerosol Lidar and Infrared Pathfinder Satellite Observation, Omar et al. 2009; EarthCARE, Illingworth et al. 2015), airborne - High Spectral Resolution Lidar (HSRL) measurements and multiwavelength Raman measurements. The CALIPSO mission uses a decision-tree based on lidar profiles and external data (Omar et al., 2009) in order to classify the aerosol load in seven aerosol subtypes, i.e., clean continental, clean, maritime, dust, polluted continental, polluted dust, smoke, and dusty maritime. The upcoming mission of EarthCARE will depend on the high-spectral-resolution lidar products for aerosol classification. The aerosol intensive properties combined with observations of the spectral aerosol optical depth will constitute the basic input for the aerosol-type determination (Wandinger et al., 2016). An aerosol classification scheme from HSRL aerosols measurements has been introduced by Burton et al. (2012). Their technique applies an objective multivariate analysis using lidar intensive properties (i.e., the particle linear depolarization ratio at 532 nm, the particle lidar ratio at 532 nm, the backscatter-related 532- to-1064nm color ratio, and the ratio of particle linear depolarization ratios at 1064 and 532 nm) and is able to detect 8 aerosol types: smoke, fresh smoke, urban, polluted maritime, maritime, dusty mix, pure dust and ice.

Several other approaches have been developed based on of the information provided by multispectral data of ground based measurements. EARLINET, for example, is a well structured network of advanced laser remote sensing stations with the main purpose of understanding the horizontal and vertical distribution of aerosols on the European scale. The EARLINET data have been extensively used not only for climatological studies (e.g., Matthias et al., 2004; Mattis et al., 2004; Amiridis2005), but also for studies on Saharan dust outbreaks (e.g., Ansmann et al., 2003; Balis et al., 2004; Papayannis et al., 2008; Tesche et al., 2009b; Mona et al., 2014 Biniotoglou et al., 2015), volcanic eruptions (e.g., Pappalardo et al., 2004; Sawamura et al., 2012; Pappalardo et al., 2013) and biomass burning events (e.g., Balis et al., 2003; Tesche et al., 2011; Nicolae et al., 2013).

Efforts for detailed knowledge of the aerosol sources have been conducted in the framework of EARLINET, focusing on the aerosol characterization and typing. For example, Müller et al. (2007) presented for the first time a statistical analysis of lidar ratios for almost all climatically relevant aerosol types based solely on Raman lidar measurements. The analysis covered the most important aerosol types such as maritime particles, desert dust particles and aged biomass-burning smoke. Lidar depolarization measurements have also been used to differentiate between different types of aerosols, since they constitute an indicator of the sphericity of particles. Tesche et al., (2009) separate the optical properties of desert dust and biomass burning particles using multiwavelength Raman and depolarization measurements. Methods for fine and coarse mode separation for dust outbreak cases, using the 532 nm particle depolarization ratio have also been developed (e.g., Ansmann et al., 2012). Ad-



ditionally, combined measurements of the lidar ratio from ground-based Raman lidars along with aerosol depolarization values and the size-sensitive Ångström exponent, were proved to be a useful tool for the separation of aerosol types as shown by Groß et al. (2011). Furthermore, the combined use of lidar observations and transport model simulations permit the discrimination of desert dust and volcanic ash particles that typically have the same optical characteristics. Simultaneous observations of  
5 desert dust and ash particles were made during the Eyjafjallajökull volcanic eruption in 2010 and the methodology for the type discrimination was presented by Mona et al. (2012); and Pappalardo et al. (2013).

In this article, a first attempt of comparing and evaluating two classification tools that provide near-real-time aerosol typing information for the lidar profiles of Thessaloniki, developed within EARLINET is presented. The article is structured as follows: Thessaloniki EARLINET lidar station is presented in Sect. 2. The two automatic aerosol classification methods and the  
10 methodology used to characterize the layers in four basic aerosol types (i.e., desert, smoke, maritime, continental) are presented in Sect. 3. In Sect. 4 the accuracy of the algorithms is tested by comparison with pre-classified case studies and an evaluation for the whole period under study is also presented. The summary and the conclusions of this article are presented in Sect. 5.

## 2 Lidar system and measurement site

The Thessaloniki lidar system (THELISYS) is operated and maintained by the Laboratory of Atmospheric Physics that is  
15 located in the Physics Department of the Aristotle University of Thessaloniki ( $40.5^{\circ} N, 22.9^{\circ} E, 50m$ ). THELISYS is used for the detection of aerosol particles as a part of EARLINET (Bosenberg et al., 2003; Pappalardo et al., 2014) since 2000 and now is part of the Aerosols, Clouds, and Trace gases Research InfraStructure (ACTRIS; [www.actris.eu/](http://www.actris.eu/)). Systematic measurements are performed, following EARLINET's schedule (i.e., every Monday morning, and every Monday and Thursday evening after the sunset). Additional measurements are performed during Saharan dust outbreaks, smoke advection from biomass burning,  
20 volcanoes, and CALIPSO correlative measurements. The current setup of THELISYS includes three elastic backscatter channels at 355 nm, 532 nm and 1064 nm, two nitrogen Raman channels at 387 nm and 607 nm and two depolarization channels. These two channels have been added to measure the cross and parallel polarized signal at 532 nm, but due to technical issues the particle depolarization ratio is currently not available. A detailed description of THELISYS can be found in Amiridis et al. (2005). Data from THELISYS are regularly analysed and quality assured and are publically available at [www.earlinet.org](http://www.earlinet.org).

Thessaloniki is in a location where many different types of aerosols coexist (Amiridis et al., 2009; Giannakaki et al., 2010; Siomos et al., 2018). Dust events are dominant during summer above 1.5 km and in autumn below 1.5 km as shown by Siomos et al., (2018). Marinou et al. (2017), also, used CALIPSO data and confirmed the existence of dust plumes during advection episodes over 2 km in summer. Similarly, the most intense biomass burning episodes tend to occur during summer in the free  
30 troposphere and are probably associated to wildfires rather than agricultural fires that tend to be predominant during spring and autumn (Siomos et al., 2018). Continental layers observed over Thessaloniki station are attributed to mixtures of anthropogenic pollution and particles from natural sources and even mixtures of maritime aerosol. Therefore, Thessaloniki is well suited for aerosol typing studies and for the investigation of the performances of different aerosol typing algorithms.



### 3 Aerosol Typing Methods

The two automatic aerosol typing methods require only lidar data with  $3\beta + 2\alpha (+1\delta)$  configuration without any use of ancillary external information. Specifically, the typing methods make use of the aerosol type-sensitive intensive properties. Multiwavelength Raman lidars have the ability to measure directly aerosol extinction and aerosol backscatter coefficient profiles in several wavelengths. Thus, a number of intensive properties can be obtained. These quantities do not depend on the aerosol load but they can be linked to the size, the chemical composition, and/or the asphericity of the particles. The investigation of these quantities is important to infer the aerosol type as discussed in many papers (e.g. Burton et al., 2012; Groß et al., 2013; Wandinger et al, 2016). The intensive properties relevant to this study are: the backscatter-related Ångström exponent, the lidar ratio, and the ratio of the lidar ratios. The aerosol backscatter coefficients at the two wavelengths ( $\lambda_1$  and  $\lambda_2$ ) are combined to give a backscatter-related aerosol Ångström exponent –  $AE(\lambda_1, \lambda_2)$ . This quantity provides information about the aerosol size. The ratio of the aerosol extinction to backscatter coefficient is called lidar ratio –  $LR_\lambda$  – and changes largely for aerosols with different chemical and physical properties. The ratio of the lidar ratios –  $LR_{\lambda_1}/LR_{\lambda_2}$  – can be used to assess the spectral dependency of the different aerosol types. It is worthwhile to mention that the particle linear depolarization ratio is an intensive property that effectively discriminates spherical and non-spherical particles in the atmosphere. However, this quantity is not used in the aerosol typing presented here.

#### 3.1 Neural network Aerosol Typing Algorithm based on Lidar data - NATALI

The NATALI (Neural network Aerosol Typing Algorithm based on Lidar data) software relies on Artificial Neural Networks (Nicolae et al., 2018). The development of this tool started in the framework of EARLINET, with the main purpose of identifying the most probable aerosol type using a combination of mean-layer intensive optical parameters (i.e., lidar ratios, Ångström exponent, color ratios) from the provided aerosol backscatter and extinction coefficient profiles of lidar systems, without any additional information. The NATALI software consists of three independent, but inter-connected modules: the input, the typing and the output module. The input module requires optical properties profiles as those measured by EARLINET stations, i.e., aerosol extinction coefficient, aerosol backscatter coefficient and particle linear depolarization ratio profiles.

In a first step, the typing module identifies the geometrical boundaries of the layers by applying the gradient method on the 1064 nm backscatter coefficient profile (Belegante et al., 2014). For every detected layer from the input module, calculations of the mean layer values of the intensive optical parameters, with respect to the signal to noise ratio and the associated uncertainties are performed (Nicolae et al., 2016). In a second step, the calculations of the optical properties for each layer are used in the typing module and compared to values obtained from a specially designed aerosol model with simulations from over 50000 synthetic cases of aerosols. A comprehensive description of the developed aerosol model can be found in Nicolae et al., (2018). The identification of the most likely probable aerosol type is then made through a voting procedure. The answer is selected based on a statistical approach and considering answers with a) high confidence, and b) stable over the uncertainty range (Nicolae et al., 2018). The Ångström Exponent at 550nm and 350nm ( $AE_{550/350}$ ), the lidar ratio at 350 nm ( $LR_{350}$ ), the lidar ratio at 550 ( $LR_{550}$ ), and color ratios  $CR_{550/350}$  and  $CR_{1000/550}$ , are used for the aerosol classification.



Depending on the availability of the particle linear depolarization ratio and the quality of the provided lidar profiles, the derived typing can be either of high resolution (AH), or low resolution with depolarization (AL) or low resolution without depolarization (BL). Pure aerosols categories, and even mixtures of three aerosols types can be obtained from the NATALI algorithm. In the high resolution typing 14 aerosol types can be distinguished (i.e., Continental, ContinentalPolluted, Dust, Maritime/CC, Smoke, Volcanic, Coastal, CoastalPolluted, ContinentalDust, ContinentalSmoke, DustPolluted, MaritimeMineral, MixedDust and MixedSmoke) when the quality of the provided optical products is high enough. In the low resolution typing 6 predominant aerosol types can be provided but with high uncertainty (i.e., Continental, Continental polluted, Smoke, Dust, Maritime and Volcanic). The low resolution typing provides 5 predominant aerosol types, either pure or mixed, when the depolarization is not provided. Finally, the output module provides the intensive optical parameters within each layer as long as their mean value and the corresponding uncertainty. The complete and detailed typing procedure derived by NATALI can be found at Nicolae et al., (2016) and at Nicolae et al., (2018).

Application of NATALI on EARLINET data samples was also conducted. Observational data from the EARLINET-CALIPSO database and measurements derived by a Raman depolarization Lidar from the Romanian National Institute for Research and Development in Optoelectronics (Belegante et al., 2011) were used. The comparison between the NATALI aerosol typing module and these observational data showed consistent results (Nicolae et al., 2018). This comparison on EARLINET data samples showed the capability of NATALI to retrieve the aerosol type from an extensive dataset, with miscellaneous quality and physical content.

### 3.2 EARLINET Mahalanobis distance-based typing algorithm

The EARLINET Mahalanobis distance-based typing algorithm is a method specifically developed for the use on the EARLINET database with a high level of flexibility in order to adapt to the different lidar set-ups and needs (Papagiannopoulos et al., 2018). The algorithm applies the Mahalanobis distance classifier (Mahalanobis, 1936) to classify observations into aerosol classes. This method demonstrated to be high performing for aerosol typing using optical properties measurements (e.g., Burton et al., 2012; Russell et al., 2014; Hamill et al., 2016).

The typing algorithm consisted of two steps. The first step is the setup of the reference dataset and the number of the aerosol classes. The reference dataset consists of well-characterized EARLINET data. The second step is the classification of unclassified data. This is done by calculating distance of an observation from already defined classes and attributing each observation to a specific class based on the minimum distance. For improving reliability of the output, a screening procedure is applied to the minimum distance. First, the minimum distance with value higher than a threshold is considered outlier and is discarded. This threshold depends on the degrees of freedom - i.e., 4 for 3 degrees of freedom. Second, an extra screening criterion is applied to almost equal values for more than one aerosol class, when the values are below the assumed threshold. For this, each distance is associated with a probability and, then, the normalized probability is required to be over 50%.

The Mahalanobis algorithm has already been evaluated in the framework of the EARLINET ACTRIS campaign during the summer 2012 (Papagiannopoulos et al., 2018). Eight reference aerosol classes which are characteristic of the following general aerosol types were initially defined: clean continental, polluted continental, pure dust, mixed dust (Dust+Maritime), polluted



dust (Dust+Smoke and/ or Dust+Polluted Continental), mixed maritime, smoke, and volcanic. The predictive accuracy of the algorithm further increased to 90% when aerosol classes that tend to reflect the same optical properties value were combined into 4 (Dust, Maritime, Polluted Continental, Clean Continental) The backscatter-related Ångström Exponent at 355nm and 1064nm ( $AE_{355/1064}$ ), the lidar ratio at 532 nm ( $LR_{532}$ ), and the ratio of the lidar ratios ( $LR_{532}/LR_{355}$ ) were used for the aerosol classification. The study concluded that the fewer aerosol classes (i.e., 4, 5, 6 classes) could provide better prediction accuracy but, nonetheless, a coarser classification. Dust showed high prediction rate, whilst the aerosol types that performed worse were the smoke and polluted continental aerosol. However, when these two categories were combined into a single aerosol class, the correct prediction increased. More detailed description about the algorithm, the reference dataset and the set of intensive parameters to separate different aerosol types can be found in Papagiannopoulos et al. (2018).

### 10 3.3 Methodology

54 Raman lidar cases of aerosol measurements (backscatter coefficient profiles at 1064nm, 532nm and 355nm, as well as the extinction coefficient profiles at 532nm and 355nm ) over Thessaloniki during the period 2012-2015 were used for this study. These input parameters were processed with NATALI software for the identification of the layer boundaries, the calculation of their mean intensive optical parameters and their corresponding uncertainties.

15 The NATALI typing was performed in the low resolution typing configuration (5 predominant aerosol types - Dust, Smoke, Continental Polluted, Continental and Maritime) since particle linear depolarization ratio measurements for Thessaloniki are not available for the study period.

20 A sensitivity analysis of NATALI input parameters to the defined aerosol layers was conducted. Three different input configurations were evaluated, concerning the layer thickness (i.e., 300 m and 600 m), the smoothing parameters (i.e., 700 number of values generated between value-uncertainty and  $\sqrt{\text{var}}$ -uncertainty for each optical parameter) and the threshold confidence (Minimum accepted confidence and Minimum agreement ratio 70% and 90%). From the processing with different settings we conclude that the typing seemed stable independently to the different input settings. Specifically, when switching from Input Settings 1 (i.e., filter window 700, layer depth 300 m and minimum accepted confidence 70%) to Input Settings 2 (i.e., filter window 1000, layer depth 600 m and minimum accepted confidence 70%), the number of layers identified is reduced, whereas by switching from Input Settings 2 to Input Settings 3 (i.e., filter window 700, layer depth 600 m and minimum accepted confidence 90%) the percentage of the identified types changes, but the aerosol type remains the same. Layers classified as Unknown (24), when one or two intensive optical parameters were outside the acceptable limits and layers classified as N/A (2) were excluded from the analysis.

30 The lidar classification consists of the main classes: large particles with medium lidar ratios (i.e., dust-like particles), large particles with low lidar ratios (i.e., marine particles), small particles with high lidar ratios (i.e., pollution and/or smoke particles) and small particles with medium lidar ratios (i.e., continental particles). The selection of four aerosol classes stems from the availability of intensive properties and the difficulty in deriving a confident classification without particle linear depolarization ratio. Regardless, the aerosol classes describe the major aerosol components. Thus, both automated typing methods are set to classify observations into 4 aerosol classes: Clean Continental, Dust, Maritime, Polluted Smoke.





The EARLINET Mahalanobis distance-based typing algorithm classes are configured as follows: Dust=dust+volcanic+mixed dust+polluted dust, Polluted Smoke=smoke+polluted continental, Clean Continental=clean continental, and Maritime=mixed maritime. The identified layer boundaries from NATALI are used for input to the EARLINET Mahalanobis distance-based typing algorithm. As, for NATALI, the low resolution typing consists of 5 aerosol classes, Smoke and Polluted Continental layers defined by NATALI were merged into Polluted Smoke (Polluted Continental + Smoke).

Desert dust layers (i.e., large with medium lidar ratio values particles) have optical properties that are considerably different from the other types, thus they are easily identified. Their big size leads to low Ångström exponent values and the reported lidar ratio at 355nm ranges from 47 to 58 sr (Siomos et al., 2018), with minimum values reported in spring in Thessaloniki. Maritime particles (i.e., large with low lidar ratio values), in contrast to desert dust particles yield low particle lidar ratio values. Polluted Smoke particles (i.e., small with high lidar ratio values particles) are highly absorbing particles exhibiting lidar ratios ranging from 52 to 73 sr (Amiridis et al., 2009; Baars et al., 2012). The highest values appear during summer period in Thessaloniki (Siomos et al., 2018). Continental particles (i.e., small with medium lidar ratio values) present low lidar ratio values, (i.e., 20–40 sr) and relatively high Ångström exponents (i.e., 1.0–2.5). The categorization of continental layers is not completely straightforward, because the continental particles can be due to different subcategories (i.e., local, continental polluted or mixtures).

#### 4 Application of the two automatic algorithms to EARLINET data - case studies

The consistency of the two automated aerosol typing algorithms on aerosol classification for two cases was first examined. A Saharan dust outbreak and a biomass burning episode over Thessaloniki station are presented below. The typing results are compared against manually typed profiles that were characterized via satellite and model simulations. Specifically, in order to identify the source of aerosol particles, backward trajectories are calculated using the Hybrid Single-Particle Lagrangian Integrated Trajectory model (HYSPPLIT; Stein et al., 2015). Additionally, the BSC-DREAM8b model (e.g., Basart et al., 2012b) was used to verify the presence of Saharan dust. Finally, fire spots from the space-based MODIS sensor (<https://firms.modaps.eosdis.nasa.gov/map/>) product FIRMS (Fire Information for Resource Management System; Giglio et al., 2016) were used to confirm the presence of smoke over of Thessaloniki.

##### 4.1 Dust Case

The first case refers to the occurrence of a dust plume over the station of Thessaloniki on 20th of May 2013. The retrieved profiles of particle backscatter and extinction coefficient, lidar ratios, and Ångström exponents are shown in Fig. 1 (a-d). The measurement is characterized by two particle layers, the first one between 0.7 and 1.6km and the second one between 2.0 and 2.7km. The dust presence was confirmed by the 7-days backward trajectories arriving at Thessaloniki on 20 of May 2013 (Fig. 1e). The trajectories indicated an event of transported Saharan dust. Additionally, the BSC-DREAM8b model was used to verify the presence of Saharan dust. The aerosol main layers and NATALI typing results are presented in Fig. 1f. For each aerosol layer (i.e., Layer A: 0.7-1.6 km and Layer B: 2-2.7 km), the mean optical properties were calculated using NATALI.



The lidar ratio value for layer A is  $45 \pm 3$  sr for 355nm and  $43 \pm 1.1$  sr for 532nm and for layer B is  $45 \pm 1.4$  sr for 355nm and  $41 \pm 1.3$  sr for 532nm correspondingly. The stability of the lidar ratio values could be considered as an indicator of homogeneity and small variability of the aerosol type within the layer. The mean  $AE_{355-532}$  was  $0.33 \pm 0.06$  for layer A and  $0.38 \pm 0.07$  for layer B respectively. The mean  $BAE_{355-532}$  and mean  $BAE_{532-1064}$  were  $0.24 \pm 0.06$  and  $0.28 \pm 0.04$  for the layer A, while the values for the layer B were  $0.13 \pm 0.07$  and  $0.06 \pm 0.04$  respectively. The retrieved values indicate the presence of coarse particles and are in agreement with the typical dust values observed over Thessaloniki (Siomos et al., 2018). NATALI typing output indicates dust layers (Fig. 1f). The EARLINET Mahalanobis distance-based typing algorithm also classifies layers A and B, as dust case (Mahalanobis distance is minimum), and Mahalanobis probability also shows good predictive performance (68% layer A and 44.6% layer B). (Fig. 1(g-h)).

## 4.2 Biomass burning episode

The second case is a biomass burning episode that occurred on 2nd September 2013. The backward trajectories from HYSPLIT in conjunction with fire spots from MODIS satellite product FIRMS indicate the biomass burning episode, transported from central Europe in the region of Thessaloniki. The optical profiles and the layers of aerosols are shown in Figure 2(a-d). The measurement is characterized by three particle layers: the first one is between 0.98km and 1.2km (Layer A), the second one between 1.7 and 2.6km (Layer B) and the third one between 2.9 and 3.5 km (Layer C). NATALI typing is presented in Fig. 2f. The mean Lidar ratio was calculated  $69 \pm 4$  for 355nm and  $70 \pm 4$  for 532nm (Layer A), for layer B was  $68 \pm 2$  sr for 355nm and  $69 \pm 2$  sr for 532nm and Layer C has values of  $66 \pm 1.4$  for 355nm and  $72 \pm 1.5$  sr for 532nm. Mean Ångström exponent for each layer was estimated at  $1.99 \pm 0.13$  (layer A),  $1.84 \pm 0.06$  (layer B) and  $1.61 \pm 0.05$  (layer C). The mean backscatter-related Ångström exponent (BAE) at 355-532nm was  $2.03 \pm 0.13$  (layer A),  $1.88 \pm 0.06$  (layer B) and  $1.79 \pm 0.05$  (layer C), while the mean backscatter-related Ångström exponent (BAE) at 532-1064nm was  $1.43 \pm 0.07$  (layer A),  $1.08 \pm 0.04$  (layer B) and  $1.18 \pm 0.03$  (layer C), respectively. These values are in accordance with the typical biomass burning values observed over Thessaloniki (Siomos et al., 2018). NATALI aerosol output (Fig. 2f) and the EARLINET Mahalanobis distance-based typing and the probability values also confirm the presence of smoke layers (Fig. 2(g-k)).

## 4.3 Aerosol classification using NATALI and EARLINET Mahalanobis distance-based typing algorithm

The complete Thessaloniki multiwavelength Raman lidar dataset for the 2012-2015 period was analyzed in terms of aerosol typing with the NATALI and the EARLINET Mahalanobis distance-based typing algorithm using the methodology reported in Sect. 3.3. For the 54 cases, 116 layers were identified by the layer identification module of NATALI. Out of 116 layers, NATALI classified 80 layers, 26 were flagged as Unknown or N/A, and 10 layers were rejected due to the fact that they were below 1 km. On the other hand, the EARLINET Mahalanobis distance-based typing algorithm successfully classified 114 layers, showing a higher identification rate. However, the comparison is made to the 80 layers that were identified by both algorithms.

The two algorithms attributed the same aerosol type to 58 layers, showing an agreement of 72.5% of the typed cases. In Fig. 3, the number of detected layers per typing class are presented for both algorithms for the whole study period. The typing procedures show the predominance of PollutedSmoke category for Thessaloniki, followed by the CleanContinental category.



Dust results in about 10% of the observed layers. Finally, although Thessaloniki is a coastal site, the maritime layers are rare, due to the mixing with other aerosol types. These results are in agreement with the findings of Siomos et al., 2018.

In particular, the agreement is high enough for the desert dust cases (12.5% and 15% for NATALI and EARLINET Mahalanobis distance-based typing algorithm, respectively). A larger difference is observed for the PollutedSmoke and CleanContinental with 15 and 17 cases of mismatch correspondingly, with a higher occurrence of PollutedSmoke cases for the EARLINET Mahalanobis distance-based typing algorithm and of CleanContinental for the NATALI algorithm.

The differences observed in Fig. 3, primarily, can be described by the different definition of the aerosol classes for the two typing methods. Moreover, the different approach by the typing methods may have an impact on the aerosol typing. For instance, for the EARLINET Mahalanobis distance-based typing algorithm the quality of the reference data and the correct definition of aerosol classes are of paramount important. It is worth noting that the aerosol model for the NATALI typing method is based on synthetic data, whereas for the EARLINET Mahalanobis distance-based typing method the aerosol model is based on EARLINET observations.

Although, each automated classification algorithm has important differences acknowledged above, the comparison showed an overall good agreement, especially for dust particles. This happens because the dust class is very well defined for both typing schemes and the physical properties are different from the other three classes. By contrast, the maritime category is defined in a different way for the two automated algorithms. The EARLINET Mahalanobis distance-based typing algorithm considers maritime layers mixed with other aerosol types, whereas for the NATALI the mixing is negligible and the aerosol type refers to pure maritime aerosol. Therefore, a direct comparison of the two methods is not possible. The absence of measurements for such kind of particle also did not allowed a direct assessment of pure marine particle synthetic data into NATALI algorithm itself. The cases typed as Maritime by NATALI were identified as Dust or CleanContinental: this is because of the different lidar ratio and backscatter Ångström related values allowed in the NATALI scheme which are recognized by the EARLINET Mahalanobis distance-based typing method as signature for Dust or CleanContinental types (Table 1). Finally, the largest number of mismatches is related to the PollutedSmoke and the CleanContinental categories.

In what follows, the NATALI aerosol model is ingested into the EARLINET Mahalanobis distance-based typing algorithm with the aim of understanding the differences of the aerosol definition. 259407 out of 424236 instances were typed by the EARLINET Mahalanobis distance-based typing algorithm. The not-typed instances were discarded by the algorithm owing to a distance-threshold filter and a distance-similarity filter (see Sect. 3.2). The results of the application of the Mahalanobis EARLINET distance-based method to the modeled reference classes of NATALI are presented in Fig. 4.

Fair agreement is found for the NATALI synthetic datasets of Dust and PollutedSmoke categories. In particular, for Dust reached agreement of 83.7%. This result is very good considering that up to 30% of the aerosol class contains mixtures. For the Polluted Smoke, the majority (58.7%) of the synthetic data is classified as PollutedSmoke. For the CleanContinental type, the agreement is poor (15%) and the majority of the instances is typed as Dust (70%). This Dust-CleanContinental mismatch is confirmed also by the 11.8% of the NATALI reference dust cases that are typed as Clean Continental by the EARLINET Mahalanobis distance-based typing method. Furthermore, 15% of the instances are classified as PollutedSmoke. Finally, the



agreement for Maritime is 23% of the cases, indicating the different class definitions as well as the big spread of the NATALI maritime model that causes the EARLINET Mahalanobis distance-based typing algorithm to misclassify those data.

Despite the important differences found on the set-up of the two methods, a very good agreement is achieved when the algorithms are applied on the EARLINET Thessaloniki dataset as shown in Fig. 5. For Dust and Polluted Smoke the accuracy reached 88.8% and 93.7% respectively. Very good performance is also found for the Clean Continental category (70%). A not satisfactory agreement is observed for the Maritime, which is the aerosol type less encountered over Thessaloniki. It is worth mentioning, here, that the addition of the particle depolarization ratio information will improve the performance of the automated typing algorithms and offer a more detailed aerosol classification.

## 5 Summary and Conclusions

10 In this study, two automated typing methods were used to obtain the best estimate of the dominant aerosol type using optical properties, measured by a multiwavelength Raman lidar over Thessaloniki. The prediction of the automatic classification methods in two study cases showed positive results when compared against manually classified EARLINET data. Additionally, all Raman measurements for the period 2012 to 2015 were analyzed and a coarse aerosol classification analysis was made and four major aerosol classes were defined as follows: 1) Dust, 2) Maritime, 3) Polluted Smoke and 4) Clean Continental.

15 Sensitivity processing in the settings of NATALI layering modules did not affect the agreement of the two algorithms which is similar (66%, 65% and 70% for each input setting correspondingly), only changes in the number of identified layers being observed. Good agreement in the aerosol classification was obtained between the two automatic procedures despite their different approaches.

Both algorithms indicated PollutedSmoke and CleanContinental as the main sources of the aerosol layers observed in 3 20 year of measurements over Thessaloniki, while Dust accounted for about 12-15% of the cases and Maritime particles were rarely observed. Good agreement is found for the Dust and Polluted Smoke (83.7% and 58.7%, respectively). Low agreement is observed for the Clean Continental and Maritime (15% and 23%, respectively), this can be ascribed to the different aerosol type definition. For instance, the NATALI algorithm considers pure marine layers while the EARLINET Mahalanobis distance-based typing algorithm considers a mixture of marine with other aerosol types.

25 The comparison of the typing results showed that the two algorithms are in a very good agreement of 88.8% for Dust, 93.7% for Polluted Smoke and 70% for Clean Continental. A poorer agreement is found for the Maritime type underlining the need for further investigation, which is partially valid also for Clean Continental.

In addition, it is worth mentioning that, as demonstrated in Nicolae et al. (2018) and Papagiannopoulos et al. (2018), the availability of the particle linear depolarization ratio improves the predictive accuracy of both methods. Its availability could 30 enhance the strength of correct predictions and lead to the increase of the number of detected types (high resolution typing) for both algorithms.



Overall, we conclude that application of these typing techniques could contribute to the improvement of the model treatment and to a better exploitation of the present and future data from satellite remote sensing for aerosol classification schemes. Further investigation on other EARLINET lidar stations needs to be conducted.

*Code availability.* The lidar data used in this study are available at <http://data.earlinet.org>. NATALI algorithm is publicly available at <http://natali.inoe.ro/resources.html/software>. The EARLINET distance-base typing algorithm and related reference datasets will be soon available at [www.earlinet.org](http://www.earlinet.org).

*Author contributions.* D. Balis, N. Siomos, and KA. Voudouri performed and processed lidar measurements during the period 2012–2015. N. Papagiannopoulos developed the EARLINET Mahalanobis distance-based typing algorithm. D. Nicolae developed the NATALI aerosol typing algorithm. K. Michailidis carried out the processing of lidar measurements with the EARLINET Mahalanobis distance-based typing algorithm. KA. Voudouri carried out the processing of lidar measurements with NATALI algorithm and prepared the figures. L. Mona reviewed parts of the comparison of the two algorithms. D. Balis is the PI of the lidar station and directed the preparation of the manuscript. KA. Voudouri prepared the manuscript with contributions from all co-authors.

*Competing interests.* The authors declare that they have no conflict of interest.

*Acknowledgements.* The research leading to these results has received funding from the European Union's Horizon 2020 Research and Innovation programme under grant agreement no. 602014, ECARS project (East European Centre for Atmospheric Remote Sensing), under grant agreement n. 654109, ACTRIS-2 project, and from the European Union's Horizon 2020 Research and Innovation programme for Societal challenges - smart, green and integrated transport, under grant agreement no. 723986, EUNADICS-AV project (European Natural Disaster Coordination and Information System for Aviation). Further financial support is provided by the Romanian Ministry of Research and Innovation throughout the Core National Program no. 33N/PN2018. Voudouri K.A acknowledges the support of the General Secretariat for Research and Technology (GSRT) and the Hellenic Foundation for Research and Innovation (HFRI), no. 294.



## References

- Amiridis, V., Balis, D. S., Kazadzis, S., Bais, A., Giannakaki, E., Papayannis, A., and Zerefos, C.: Four-year aerosol observations with a Raman lidar at Thessaloniki, Greece, in the framework of European Aerosol Research Lidar Network (EARLINET), *Journal of Geophysical Research: Atmospheres*, 110, <https://doi.org/10.1029/2005JD006190>, d21203, 2005
- 5 Amiridis, V., Balis, D. S., Giannakaki, E., Stohl, A., Kazadzis, S., Koukouli, M. E., and Zanis, P.: Optical characteristics of biomass burning aerosols over Southeastern Europe determined from UV-Raman lidar measurements, *Atmos. Chem. Phys.*, 9, 2431–2440, doi:10.5194/acp-9-2431-2009, 2009.
- Ansmann A., Bosenberg J., Chaikovskiy A., Cameron A., Eckhardt S., Eixmann R., Freudenthaler V., Ginoux P., Komguem P., Linne H., Angel Lopez Marquez M., Matthias V., Mattis I., Mitev V., Müller D., Music S., Nickovic S., Pelon J., Sauvage L., Sobolewsky P.,  
10 Srivastava M. K., Stohl A., Torres O., Vaughan G., Wandinger U., and Wiegner M.: Long-range transport of Saharan dust to northern Europe: The 11 – 16 October 2001 outbreak observed with EARLINET, *J. Geophys. Res.*, 108, (D24), 4783, doi:10.1029/2003JD003757, 2003
- Ansmann, A., Mattis, I., Müller, D., Wandinger, U., Radlach, M. and co-authors: Ice formation in Saharan dust over central Europe observed with temperature/humidity/aerosol Raman lidar. *J. Geophys. Res.* 110, doi:10.1029/2005JD005000, 2005.
- 15 Ansmann, A., Petzold, A., Kandler, K., Tegen, I., Wendisch, M., Müller, D., Weinzierl, B., Müller, T., and Heintzenberg, J.: Saharan Mineral Dust Experiments SAMUM-1 and SAMUM-2: what have we learned?, *Tellus B*, 63, doi:10.1111/j.1600-0889.2011.00555.x, 2011.
- Baars, H., Ansmann, A., Althausen, D., Engelmann, R., Heese, B., Müller, D., Artaxo, P., Paixao, M., Pauliquevis, M., and Souza, R.: Aerosol profiling with lidar in the Amazon Basin during the wet and dry season, *J. Geophys. Res.*, 117, doi:10.1029/2012JD018338, 2012.
- Baars, H., Kanitz, T., Engelmann, R., Althausen, D., Heese, B., Komppula, M., Preißler, J., Tesche, M., Ansmann, A., Wandinger, U., Lim, J.-  
20 H., Ahn, J. Y., Stachlewska, I. S., Amiridis, V., Marinou, E., Seifert, P., Hofer, J., Skupin, A., Schneider, F., Bohlmann, S., Foth, A., Bley, S., Pfüller, A., Giannakaki, E., Lihavainen, H., Viisanen, Y., Hooda, R. K., Pereira, S. N., Bortoli, D., Wagner, F., Mattis, I., Janicka, L., Markowicz, K. M., Achtert, P., Artaxo, P., Pauliquevis, T., Souza, R. A. F., Sharma, V. P., van Zyl, P. G., Beukes, J. P., Sun, J., Rohwer, E. G., Deng, R., Mamouri, R.-E., and Zamorano, F.: An overview of the first decade of PollyNET: an emerging network of automated Raman-polarization lidars for continuous aerosol profiling, *Atmospheric Chemistry and Physics*, 16, 5111–5137, doi:10.5194/acp-16-5111-2016,  
25 <http://www.atmos-chem-phys.net/16/5111/2016/>, 2016.
- Balis D., Amiridis V., Zerefos C., Gerasopoulos E., Andreae M., Zanis P., Kazantzidis A., Kazadzis S., and Papayannis A.: Raman lidar and sun photometric measurements of aerosol optical properties over Thessaloniki, Greece during a biomass burning episode, *Atmospheric Environment*, Volume 37, Issue 32, 2003, Pages 4529-4538, ISSN 1352-2310, [https://doi.org/10.1016/S1352-2310\(03\)00581-8](https://doi.org/10.1016/S1352-2310(03)00581-8), 2003.
- Balis D., Amiridis V., Nickovic S., Papayannis A., and Zerefos C.: Optical properties of Saharan dust layers as detected by a Raman lidar at  
30 Thessaloniki, Greece, *Geophysical Research Letters - GEOPHYS RES LETT*. 311. 10.1029/2004GL019881, 2004.
- Basart, S., Pérez, C., Nickovic, S., Cuevas, E., and Baldasano, J.: Development and evaluation of the BSC-DREAM8b dust regional model over Northern Africa, the Mediterranean and the Middle East, *Tellus B*, 64, 18539, <https://doi.org/10.3402/tellusb.v64i0.18539>, 2012b.
- Belegante, L., Talianu, C., Nemuc, A., and Nicolae, D.: Detection of local weather events from multiwavelength lidar measurements during the EARLI09 campaign, *Rom. J. Phys.*, 56(3–4), 484–494, 2011.
- 35 Belegante, O., Nicolae, D., Nemuc, A., Talianu, C. and Derognat, C., Retrieval of the boundary layer height from active and passive remote sensors. Comparison with a NWP model, *Acta Geophysica*, 62 (2), 276-289, doi:10.2478/s11600-013-0167-4, 2014.



- Biniotoglou, I., Basart, S., Alados-Arboledas, L., Amiridis, V., Argyrouli, A., Baars, H., Baldasano, J. M., Balis, D., Belegante, L., Bravo-Aranda, J. A., Burlizzi, P., Carrasco, V., Chaikovsky, A., Comerón, A., D'Amico, G., Filioglou, M., Granados-Muñoz, M. J., Guerrero-Rascado, J. L., Ilic, L., Kokkalis, P., Maurizi, A., Mona, L., Monti, F., Muñoz-Porcar, C., Nicolae, D., Papayannis, A., Pappalardo, G., Pejanovic, G., Pereira, S. N., Perrone, M. R., Pietruczuk, A., Posyniak, M., Rocadenbosch, F., Rodríguez-Gómez, A., Sicard, M., Siomos, N., Szkop, A., Terradellas, E., Tsekeri, A., Vukovic, A., Wandinger, U., and Wagner, J.: A methodology for investigating dust model performance using synergistic EARLINET/AERONET dust concentration retrievals, *Atmos. Meas. Tech.*, 8, 3577-3600, <https://doi.org/10.5194/amt-8-3577-2015>, 2015.
- Bosenberg, J., Matthias, V., Amodeo, A., et al.: EARLINET: A European Aerosol Research Lidar Network to Establish an Aerosol Climatology', Report of the Max-Planck-Institute for Meteorology No. 348, 16–39, 2003.
- Burton, S. P., Ferrare, R. A., Hostetler, C. A., Hair, J. W., Rogers, R. R., Obland, M. D., Butler, C. F., Cook, A. L., Harper, D. B., and Froyd, K. D.: Aerosol classification using airborne High Spectral Resolution Lidar measurements – methodology and examples, *Atmospheric Measurement Techniques*, 5, 73–98, doi:10.5194/amt-5-73-2012, <http://www.atmos-meas-tech.net/5/73/2012/>, 2012.
- Giannakaki, E., Balis, D. S., Amiridis, V., and Zerefos, C.: Optical properties of different aerosol types: seven years of combined Raman-elastic backscatter lidar measurements in Thessaloniki, Greece, *Atmospheric Measurement Techniques*, 3, 569–578, <https://doi.org/10.5194/amt-3-569-2010>, 2010.
- Giglio L., Schroeder, W., Justice, C.O. : The collection 6 MODIS active fire detection algorithm and fire products. *Remote Sensing of Environment*, 178, 31-41, 2016.
- Groß, S., Tesche, M., Freudenthaler, V., Toledano, C., Wiegner, M., Ansmann, A., Althausen, D., and Seefeldner, M.: Characterization of Saharan dust, Maritime aerosols and mixtures of biomass-burning aerosols and dust by means of multi-wavelength depolarization and Raman lidar measurements during SAMUM 2, *Tellus B*, 63, 706–724, doi:10.1111/j.1600-0889.2011.00556.x, 2011.
- Groß, S., Esselborn, M., Weinzierl, B., Wirth, M., Fix, A., and Petzold, A.: Aerosol classification by airborne high spectral resolution lidar observations, *Atmospheric Chemistry and Physics*, 13, 2487–2505, doi:10.5194/acp-13-2487-2013, <http://www.atmos-chem-phys.net/13/2487/2013/>, 2013.
- Hamill, P., et al.: An AERONET-based aerosol classification using the Mahalanobis distance, *Atmos. Env.*, 140, 213-233, doi:10.1016/j.atmosenv.2016.06.002, 2016.
- Illingworth, A. J., Barker, H. W., Beljaars, A., Ceccaldi, M., Chepfer, H., Cole, J., Delanoë, J., Domenech, C., Donovan, D. P., Fukuda, S., Hirakata, M., Hogan, R. J., Huenerbein, A., Kollias, P., Kubota, T., Nakajima, T., Nakajima, T. Y., Nishizawa, T., Ohno, Y., Okamoto, H., Oki, R., Sato, K., Satoh, M., Shephard, M., Wandinger, U., Wehr, T., and Van Zadelhoff, G.-J.: THE EARTHCARE SATELLITE: The next step forward in global measurements of clouds, aerosols, precipitation and radiation, *Bulletin of the American Meteorological Society (BAMS)*, p. (in press), doi:10.1175/BAMS-D-12-00227.1, 2015.
- Mahalanobis, P. C.: On the generalized distance in statistics. *Proceedings of the National Institute of Science of India*, 12, 49–55, 1936.
- Marinou, E., Amiridis, V., Biniotoglou, I., Tsikerdekis, A., Solomos, S., Proestakis, E., Konsta, D., Papagiannopoulos, N., Tsekeri, A., Vlastou, G., Zanis, P., Balis, D., Wandinger, U., and Ansmann, A.: Three-dimensional evolution of Saharan dust transport towards Europe based on a 9-year EARLINET-optimized CALIPSO dataset, *Atmospheric Chemistry and Physics*, 17, 5893–5919, <https://doi.org/10.5194/acp-17-5893-2017>, 2017.
- Matthias V., and Bosenberg J.: Aerosol climatology for the planetary boundary layer derived from regular lidar measurements, *Atmospheric Research*, Volume 63, Issues 3–4, Pages 221-245, ISSN 0169-8095, [https://doi.org/10.1016/S0169-8095\(02\)00043-1](https://doi.org/10.1016/S0169-8095(02)00043-1), 2002.



- Mattis, I., Ansmann, A., Mueller, D., Wandinger, U. & Althausen, D.: Multiyear aerosol observations with dual-wavelength Raman lidar in the framework of EARLINET, *Journal of Geophysical Research: Atmospheres*, vol 109, no. D13, D13203. DOI: 10.1029/2004jd004600, 2004.
- 5 Mona, L., Amodeo, A., D'Amico, G., Giunta, A., Madonna, F., and Pappalardo, G.: Multi-wavelength Raman lidar observations of the Eyjafjallajökull volcanic cloud over Potenza, southern Italy, *Atmos. Chem. Phys.*, 12, 2229-2244, <https://doi.org/10.5194/acp-12-2229-2012>, 2012.
- Mona, L., Papagiannopoulos, N., Basart, S., Baldasano, J., Biniotoglou, I., Cornacchia, C., and Pappalardo, G.: EARLINET dust observations vs. BSC-DREAM8b modeled profiles: 12-year-long systematic comparison at Potenza, Italy, *Atmos. Chem. Phys.*, 14, 8781-8793, <https://doi.org/10.5194/acp-14-8781-2014>, 2014.
- 10 Müller, D., Ansmann, A., Mattis, I., Tesche, M., Wandinger, U., Althausen, D., and Pisani G., Aerosol-type-dependent lidar ratios observed with Raman lidar, *Journal Of Geophysical Research*, Vol. 112, D16202, doi:10.1029/2006JD008292, 2007
- Nicolae, D., Nemuc, A., Müller, D., Talianu, C., Vasilescu, J., Belegante, L., and Kolgotin, A.: Characterization of fresh and aged biomass burning events using multiwavelength Raman lidar and mass spectrometry, *J. Geophys. Res. Atmospheres*, 118, 2956-2965, <https://doi.org/10.1002/jgrd.50324>, 2013.
- 15 Nicolae D., Vasilescu J., Talianu C. and Dandocsi A.: Independent Retrieval of Aerosol Type From Lidar, *EPJ Web of Conferences* 119, 18002, <https://doi.org/10.1051/epjconf/201611918002>, 2016.
- Nicolae D., Vasilescu J., Talianu C., Biniotoglou I., Nicolae V., Andrei S., and Antonescu B.: A Neural Network Aerosol Typing Algorithm Based on Lidar Data, *Atmos. Chem. Phys. Discuss.*, <https://doi.org/10.5194/acp-2018-492>, 2018
- Nicolae D., Talianu C., Vasilescu J., Nicolae V., Stachlewska I.S.: Strengths and limitations of the NATALI code for aerosol typing from multiwavelength Raman lidar observations, *EPJ Web of Conferences* 176, 05005, <https://doi.org/10.1051/epjconf/201817605005>, 2018
- 20 Omar, A. H., Winker, D. M., Kittaka, C., Vaughan, M. A., Liu, Z., Hu, Y., Trepte, C. R., Rogers, R. R., Ferrare, R. A., Lee, K.-P., Kuehn, R. E., and Hostetler, C. A. : The CALIPSO automated aerosol classification and lidar ratio selection algorithm, *Journal of Atmospheric and Oceanic Technology*, 26, 1994, doi:10.1175/2009JTECH1231.1, <http://ams.allenpress.com/perlserv/?request=get-abstract&.doi=10.2009>.
- 25 Papagiannopoulos, N., Mona, L., Amodeo, A., D'Amico, G., Gumà Claramunt, P., Pappalardo, G., Alados-Arboledas, L., Guerrero-Rascado, J. L., Amiridis, V., Kokkalis, P., Apituley, A., Baars, H., Schwarz, A., Wandinger, U., Biniotoglou, I., Nicolae, D., Bortoli, D., Comerón, A., Rodríguez-Gómez, A., Sicard, M., Papayannis, A., and Wiegner, M.: An automatic observation-based aerosol typing method for EARLINET, *Atmos. Chem. Phys.*, 18, 15879-15901, <https://doi.org/10.5194/acp-18-15879-2018>, 2018.
- Papagiannopoulos, N., Mona, L., Alados-Arboledas, L., Amiridis, V., Baars, H., Biniotoglou, I., Bortoli, D., D'Amico, G., Giunta, A., Guerrero-Rascado, J. L., Schwarz, A., Perreira, S., Spinelli, N., Wandinger, U., Wang, X., and Pappalardo, G.: CALIPSO climatological products: evaluation and suggestions from EARLINET, *Atmos. Chem. Phys.*, 16, 2341-2357, doi:10.5194/acp-16-2341-2016, 2016a.
- 30 Papagiannopoulos, N., Mona, L., and Pappalardo, G.: Aerosol classification using EARLINET measurements for an intensive observational period, vol. 18, European Geosciences Union, General Assembly, 2016b.
- Papayannis, A., et al., Systematic lidar observations of Saharan dust over Europe in the frame of EARLINET (2000-2002), *J. Geophys. Res.*, 113, D10204, doi: 10.1029/2007JD009028, 2008.
- Pappalardo, G., A. Amodeo, L. Mona, M. Pandolfi, N. Pergola, and V. Cuomo (2004), Raman lidar observations of aerosol emitted during the 2002 Etna eruption, *Geophys. Res. Lett.*, 31, L05120, doi: 10.1029/2003GL019073.





- Pappalardo, G., Mona, L., D'Amico, G., Wandinger, U., Adam, M., Amodeo, A., Ansmann, A., Apituley, A., Alados Arboledas, L., Balis, D., Boselli, A., Bravo-Aranda, J. A., Chaikovskiy, A., Comeron, A., Cuesta, J., De Tomasi, F., Freudenthaler, V., Gausa, M., Giannakaki, E., Giehl, H., Giunta, A., Grigorov, I., Groß, S., Haefelin, M., Hiebsch, A., Iarlori, M., Lange, D., Linné, H., Madonna, F., Mattis, I., Mamouri, R.-E., McAuliffe, M. A. P., Mitev, V., Molero, F., Navas-Guzman, F., Nicolae, D., Papayannis, A., Perrone, M. R., Pietras, C., Pietruczuk, A., Pisani, G., Preißler, J., Pujadas, M., Rizi, V., Ruth, A. A., Schmidt, J., Schnell, F., Seifert, P., Serikov, I., Sicard, M., Simeonov, V., Spinelli, N., Stebel, K., Tesche, M., Trickl, T., Wang, X., Wagner, F., Wiegner, M., and Wilson, K. M.: Four-dimensional distribution of the 2010 Eyjafjallajökull volcanic cloud over Europe observed by EARLINET, *Atmospheric Chemistry and Physics*, 13, 4429–4450, doi:10.5194/acp-13-4429-2013, 2013.
- Pappalardo G., Amodeo A., Apituley A., Comeron A., Freudenthaler V., Linne H., Ansmann A., Bosenberg J., D'Amico G., Mattis I., Mona L., Wandinger U., Amiridis V., Alados-Arboledas L., Nicolae D., and Wiegner M.: EARLINET: towards an advanced sustainable European aerosol lidar network, 2014.
- Pérez, C., Nickovic, S., Pejanovic, G., Baldasano, J. M., and Özsoy, E.: Interactive dust-radiation modeling: A step to improve weather forecasts, *J. Geophys. Res.-Atmos.*, 111, d16206, <https://doi.org/10.1029/2005JD006717>, 2006b.
- Preißler, J., Wagner, F., Guerrero-Rascado, J. L., and Silva, A. M.: Two years of free-tropospheric aerosol layers observed over Portugal by lidar, *J. Geophys. Res. Atmos.*, 118, 3676–3686, doi:10.1002/jgrd.50350, 2013.
- Russell, P.B., et al.: A multiparameter aerosol classification method and its application to retrievals from spaceborne polarimetry, *J. Geophys. Res. Atmos.*, 119, 9838–9863, doi:10.1002/2013JD021411, 2014.
- Sawamura P., Vernier J.P., Barnes J.E., Berkoff T.A., Welton E.J., Alados-Arboledas L., Navas-Guzmán F., Pappalardo G., Mona L., Madonna F., Lange D., Sicard M., Godin-Beekmann S., and Payen G., Wang Z., Hu S., Tripathi S.N., and Cordoba-Jabonero C., and Hoff R.M.: Stratospheric AOD after the 2011 eruption of Nabro volcano measured by lidars over the Northern Hemisphere, *Environmental Research Letters*, 7 034013, 2012
- Schmeisser, L., Andrews, E., Ogren, J. A., Sheridan, P., Jefferson, A., Sharma, S., Kim, J.E., Sherman, J. P., Sorribas M., Kalapov, I., Arsov, T., Angelov, C., Mayol-Bracero, O.L., Labuschagne, C., Kim, S.W., Hoffer, A., Lin, N.H., Chia, H.P., Bergin, M., Sun, J., Liu, P., and Wu, H., Classifying aerosol type using in situ surface spectral aerosol optical properties, *Atmos. Chem. Phys.*, 17, 12097–12120, <https://doi.org/10.5194/acp-17-12097-2017>, 2017.
- Siomos, N., Balis, D. S., Voudouri, K. A., Giannakaki, E., Filioglou, M., Amiridis, V., Papayannis, A., and Fragkos, K.: Are EARLINET and AERONET climatologies consistent? The case of Thessaloniki, Greece, *Atmos. Chem. Phys.*, 18, 11885–11903, <https://doi.org/10.5194/acp-18-11885-2018>, 2018.
- Stein, A.F., Draxler, R.R., Rolph, G.D., Stunder, B.J.B., Cohen, M.D., and Ngan, F.: NOAA's HYSPLIT atmospheric transport and dispersion modeling system, *Bull. Amer. Meteor. Soc.*, 96, 2059–2077, <http://dx.doi.org/10.1175/BAMS-D-14-00110.1>, 2015
- Rolph, G., Stein, A., and Stunder, B.: Real-time Environmental Applications and Display sYstem: READY. *Environmental Modelling & Software*, 95, 210–228, 2017.
- Tesche, M., A. Ansmann, D. Müller, D. Althausen, R. Engelmann, V. Freudenthaler, and S. Groß, Vertically resolved separation of dust and smoke over Cape Verde using multiwavelength Raman and polarization lidars during Saharan Mineral Dust Experiment 2008, *J. Geophys. Res.*, 114, D13202, doi:10.1029/2009JD011862, 2009a.
- Tesche, M., Ansmann, A., Müller, D., Althausen, D., Mattis, I., Heese, B., Freudenthaler, V., Wiegner, M., Esselborn, M., Pisani, G., and Knippertz, P.: Vertical profiling of Saharan dust with Raman lidars and airborne HSRL in southern Morocco during SAMUM, *Tellus B*, 61, 144–164, <https://doi.org/10.1111/j.1600-0889.2008.00390.x>, 2009b.



Tesche, M., Detlef, M., Groß, S., Ansmann, A., Althausen, D., Freudenthaler, V., Weinzierl, B., Veira, A., and Petzold, A.: Optical and microphysical properties of smoke over Cape Verde inferred from multiwavelength lidar measurements, *Tellus B*, 63, 677–694, <https://doi.org/10.3402/tellusb.v63i4.16362>, 2011a.

5 Tesche, M., Groß, S., Ansmann, A., Müller, D., Althausen, D., Freudenthaler, V., and Esselborn, M.: Profiling of Saharan dust and biomass-burning smoke with multiwavelength polarization Raman lidar at Cape Verde, *Tellus B*, 63, <http://www.tellusb.net/index.php/tellusb/article/view/16360>, 2011b.

Wandinger, U., Baars, Holger, Engelmann, R., Hünerbein, A., Horn, S., Kanitz, T., Donovan, D., van Zadelhoff, G.-J., Daou, D., Fischer, J., von Bismarck, J., Filipitsch, F., Docter, N., Eisinger, M., Lajas, D., and Wehr, T.: HETEAC: The Aerosol Classification Model for Earth-CARE, *EPJ Web of Conferences*, 119, 01 004, doi:10.1051/epjconf/201611901004, <http://dx.doi.org/10.1051/epjconf/201611901004>,  
10 2016.


**Table 1.** Mean aerosol optical properties of the reference aerosol types used on the two automated algorithms.

NATALI	$AE_{550/350}$	$LR_{350}$	$LR_{550}$
Dust (D)	0.88–0.92	43–46	44–49
Continental polluted (CPolluted)	1.17–1.34	55–75	62–74
Smoke (S)	1.15–1.31	56–72	81–92
Clean Continental (CC)	1.17–1.29	43–54	52–53
Maritime (MM)	-0.26–0.21	13–32	19–25
EARLINET Mahalanobis distance-based typing algorithm	$AE_{355/1064}$	$LR_{532}$	$LR_{532}/LR_{355}$
Dust (D)	0.2–0.8	44–62	0.86–1.34
PollSmoke (PS)	1.1–1.5	52–82	0.68–1.12
Clean Continental (CC)	0.8–1.4	35–47	0.6–1.0
Maritime (MM)	0.7–1.1	16–32	0.8–1.0

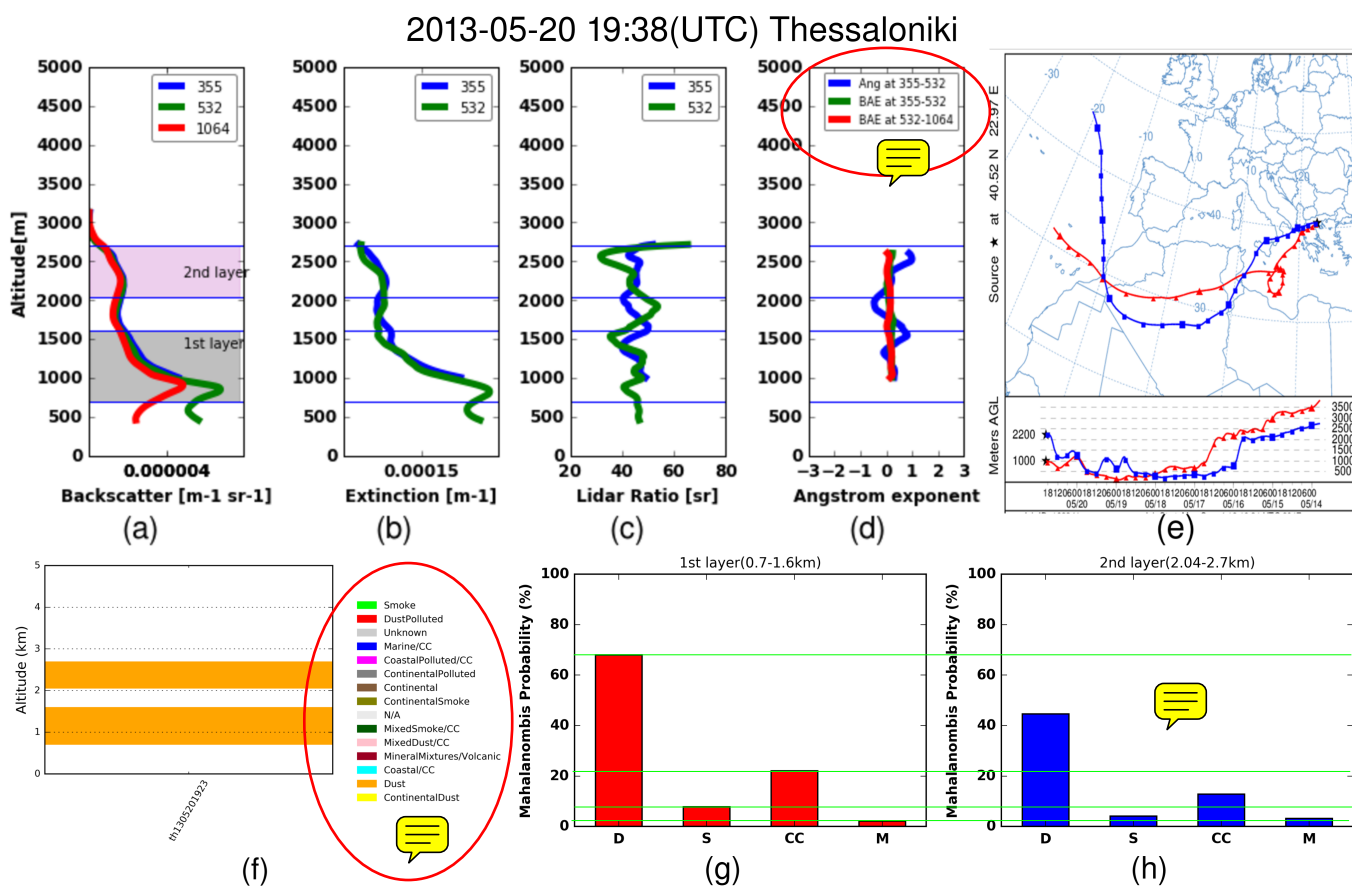


**Figure 1.** Vertical profiles of aerosol optical properties for Thessaloniki on 20th May 2013. (a) Backscatter coefficient at 355nm, 532nm and 1064nm, (b) extinction coefficient at 355 nm and 532nm, (c) Lidar Ratio, (d) Ångström exponent, (e) seven-days HYSPLIT backward trajectories arriving at Thessaloniki at each detected layer height, (f) aerosol main layers typed by NATALI and (g,h) EARLINET Mahalanobis distance-based typing algorithm probability for each detected layer.

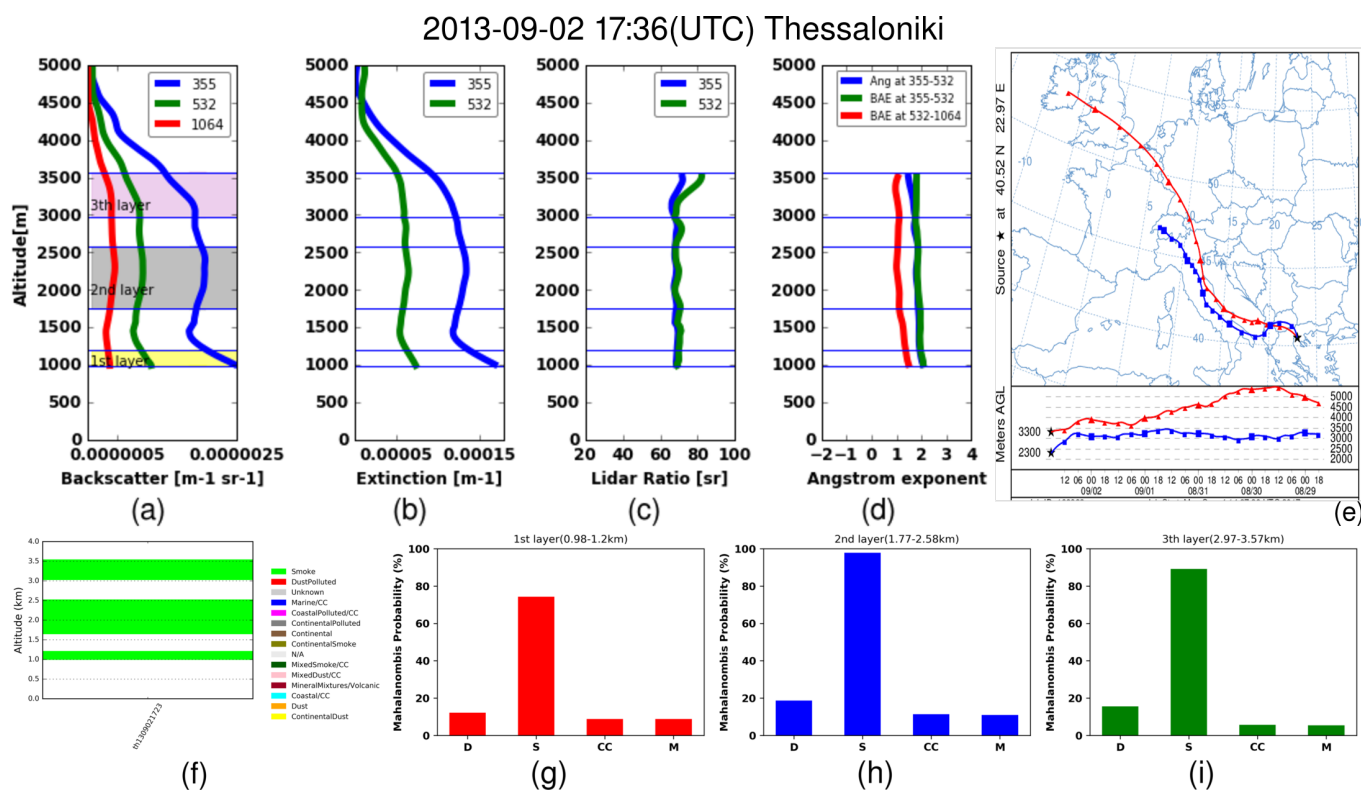


**Figure 2.** Vertical profiles of aerosol optical properties for Thessaloniki on 2nd of September 2013. (a) Backscatter coefficient profiles at 355nm, 532nm and 1064nm, (b) extinction coefficient profiles at 387nm and 607nm, (c) Lidar Ratio, (d) Ångström exponent, (e) seven-days backward trajectories arriving at Thessaloniki at each detected layer height, (f) aerosol main layers typed by NATALI, and (g,h,i) EARLINET Mahalanobis distance-based typing algorithm probability for each detected layer.

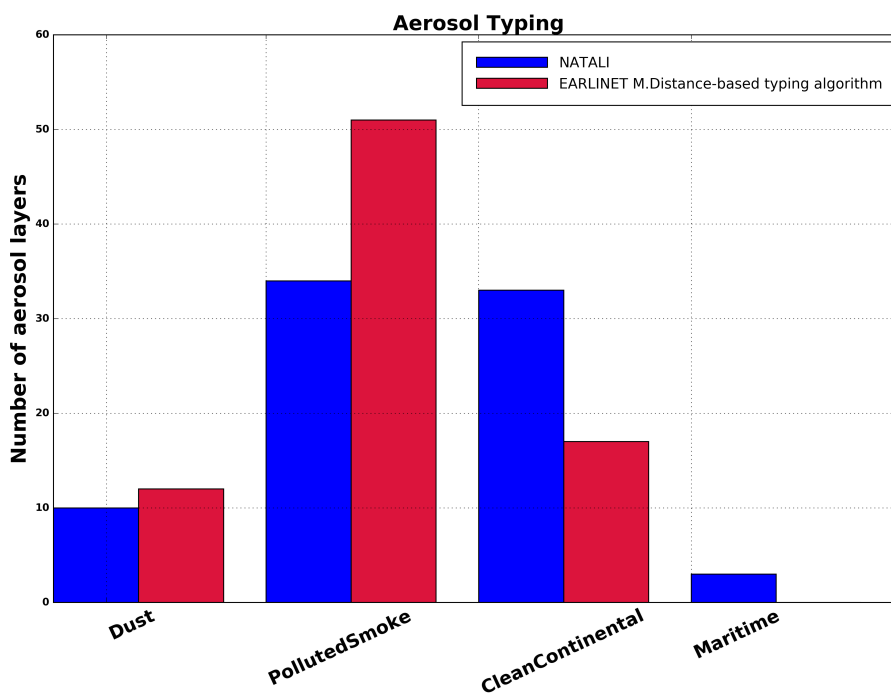


**Figure 3.** Bar plots showing the number of detected layers per aerosol class from both algorithms for Thessaloniki station for the period under study (2012–2015).

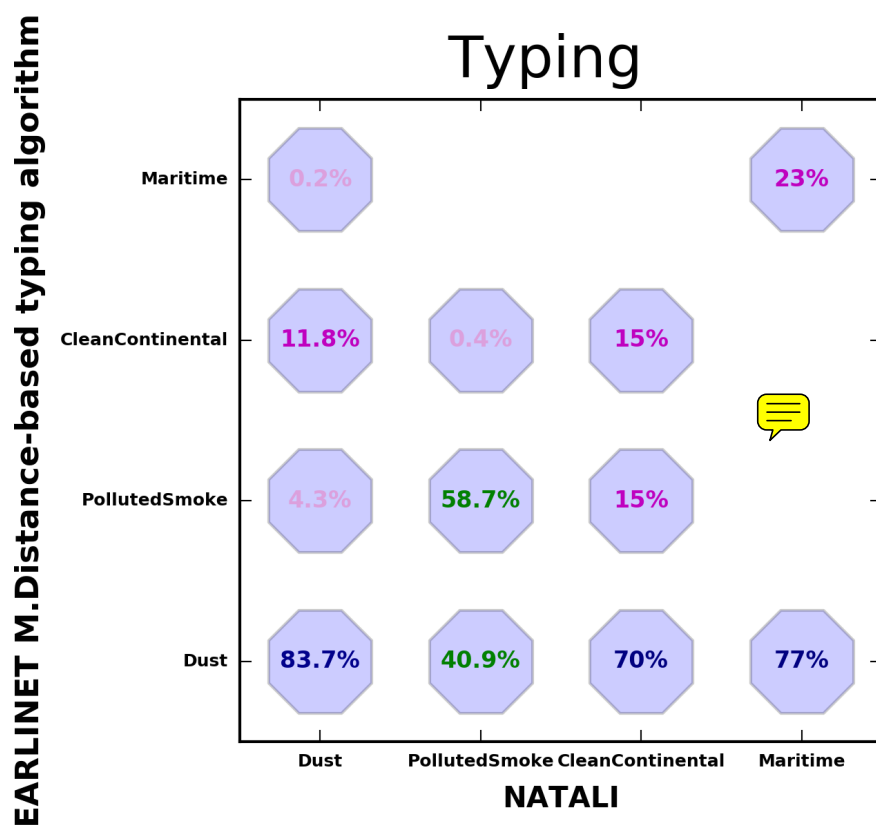


**Figure 4.** Prediction accuracy for each aerosol class derived by the applying of the EARLINET Mahalanobis distance-based typing algorithm to NATALI modeled data set.

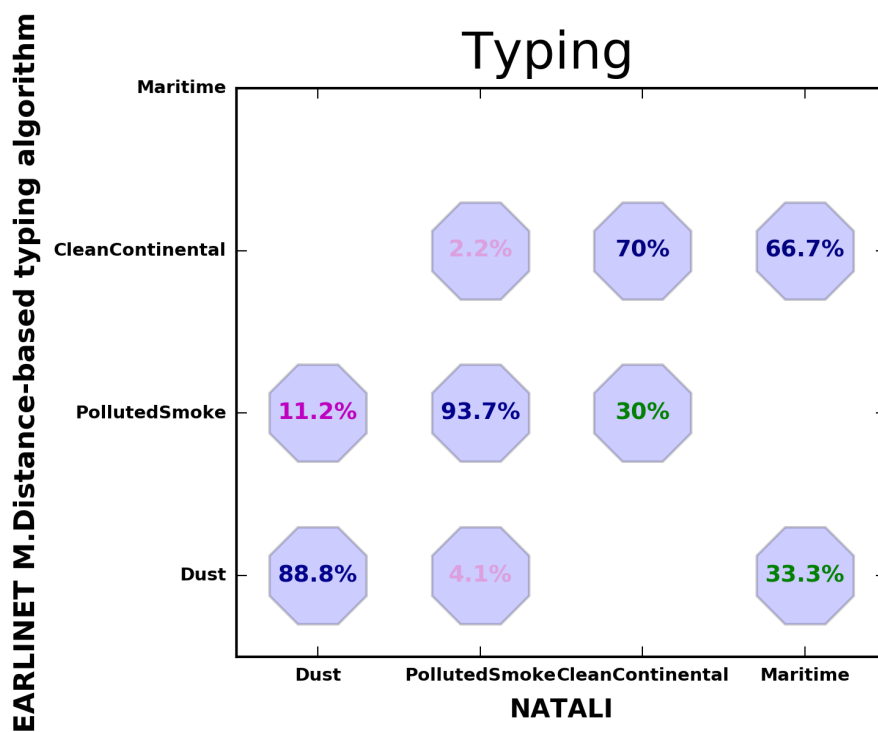


**Figure 5.** Prediction accuracy for each aerosol class derived by the two algorithms for Thessaloniki station for the period under study.